# Gap solitons in optical lattices embedded into nonlocal media

YuanYao Lin,[1] Chandroth P. Jisha,[1] Ching-Jen Jeng,[1] Ray-Kuang Lee,[1] and Boris A. Malomed[2]
[1]*Institute of Photonics Technologies, National Tsing-Hua University, Hsinchu 300, Taiwan*
[2]*Department of Physical Electronics, School of Electrical Engineering, Faculty of Engineering, Tel Aviv University, Tel Aviv 69978, Israel*
(Received 15 March 2010; published 2 June 2010)

We analyze the existence, stability, and mobility of gap solitons (GSs) in a periodic photonic structure built into a nonlocal self-defocusing medium. Counterintuitively, the GSs are supported even by a highly nonlocal nonlinearity, which makes the system quasilinear. Unlike local models, the variational approximation predicts the GSs in good agreement with numerical findings due to the suppression of undulating tails of the solitons.

DOI: 10.1103/PhysRevA.81.063803 PACS number(s): 42.65.Tg, 42.65.Sf, 42.70.Qs

## I. INTRODUCTION

Solitons are self-guided wave packets propagating in nonlinear media that maintain their self-trapped shape. In particular, optical solitons are supported by the balance between the material nonlinearity and diffraction in the spatial domain or dispersion in the temporal domain [1]. As concerns spatial solitons in planar waveguides, it is well known that the self-focusing Kerr nonlinearity supports bright ones, while a defocusing nonlinearity admits dark solitons. Even in the absence of integrability, solitons readily feature quasiparticle collisions, with the outcome depending on the relative phase between them. These properties suggest using solitons in various applications for all-optical data-processing schemes and telecommunication systems [2].

Efficient control of the transmission and localization of light may be provided by photonic crystals (PhCs) built as structures with periodic modulation of the refractive index (RI). They open ways to tailor the dispersion, diffraction, and routing of electromagnetic waves [3]. Nonlinear PhCs, composed of appropriate materials, have revealed a wealth of nonlinear optical phenomena, including the self-trapping of localized modes in the form of the gap solitons (GSs) [4–6]. These modes can be formed in self-focusing and defocusing media alike, due to the possibility of the change in the sign of the effective dispersion and diffraction in PhCs [7]. Experimentally, GSs were first created in the temporal domain as solitons in a short piece of a fiber Bragg grating [8]. Technologies based on the use of reconfigurable (photoinduced) lattices, that have been implemented in photorefractive crystals [9] and nematic liquid crystals [10], offer new ways to control GSs in the spatial domain by varying the lattice depth and spacings.

Combining the benefits of PhCs and solitons, GSs have considerable potential for use in photonics. GSs of matter waves have also been theoretically studied [11] and experimentally created [12] in Bose-Einstein condensates formed by atoms with repulsive interactions trapped in optical-lattice potentials. Bifurcations and stability of optical GSs were analyzed in PhCs with the local Kerr nonlinearity [13]. However, the limited mobility of GSs in the transverse directions, due to their pinning to the underlying lattice potentials [14], is an obstacle to the use of GSs in switching and routing operations [15,16].

Recently, it has been predicted that solitons supported by a *nonlocal* nonlinearity, self-focusing or defocusing, in combination with effective diffraction induced by either the total internal reflection (ordinary solitons) [17] or band-gap spectrum [18], may move much easier across the lattice. Nonlocal effects come to play an important role as the characteristic correlation radius of the medium's response function becomes comparable to the transverse width of the wave packet [19]. Experimental observations of nonlocal responses have been demonstrated in various media, including photorefractive crystals [20], nematic liquid crystals [21], and thermo-optical materials [22,23]. The nonlocal nonlinearity induces new features in the wave dynamics, modifying the underlying modulational [24], azimuthal [25], and transverse [26] instabilities. Suppression of the collapse of multidimensional solitons [27], a change of interactions between them [28], the formation of soliton bound states [29], the merger of colliding solitons into a standing wave [30], and families of dark-bright soliton pairs [31] were also predicted recently.

The nonlocality is known to improve the stability of solitons due to the diffusion mechanism of the underlying nonlinearity. In the limit of strongly nonlocal nonlinearity, the system becomes an effectively linear one [32]. In such an extreme limit, the existence of GSs (for the defocusing sign of the nonlinearity) is questionable. In this work, we identify families of bright on-site and off-site GSs in self-defocusing nonlinear media by means of numerical methods and analytical methods. With the infinite range of the nonlocality, we demonstrate the existence of spatial GSs with a finite beam width. The analytical consideration is based on the variational approximation (VA) with a Gaussian ansatz, which is similar to how it was applied to the matter-wave GSs in Refs. [33,34]. Unlike the case of the local defocusing nonlinearity, in the nonlocal case the Gaussian ansatz works well not only deep inside of the band gap but also close to its edge. The stability and mobility of the GS families in the nonlocal medium are investigated too.

## II. THE MODEL AND NUMERICAL RESULTS FOR GAP SOLITONS

We consider a wave packet propagating along axis $z$ in a PhC structure embedded into a medium with the self-defocusing cubic nonlocal nonlinearity. A model widely adopted for the description of such media is [24,35]

$$i\frac{\partial \Psi}{\partial z} = -\frac{1}{2}\frac{\partial^2}{\partial x^2}\Psi + V(x)\Psi + n\Psi, \tag{1}$$

$$n - d\frac{\partial^2}{\partial x^2}n = |\Psi|^2, \tag{2}$$

 

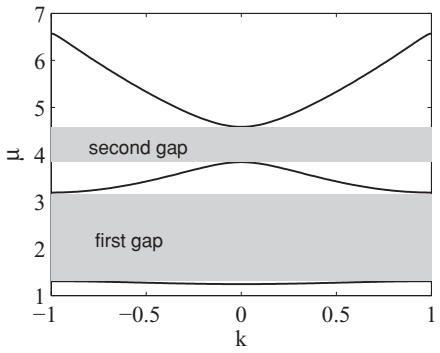


FIG. 1. Typical example of the spectrum, with quasi–wave number $k$, induced by the linearized version of Eq. (3), with $V_0 = 4$. Shaded areas are covered by the band gaps.

where $\Psi$ is the amplitude of the electromagnetic wave, $x$ is the transverse coordinate, $n(x,z)$ is a perturbation of the local RI corresponding to the intensity-response function with an exponential kernel, and $d$ is a parameter which determines the degree of the nonlocality of the response. All the physical quantities and spatial coordinates are made dimensionless by normalization procedures with respect to the input beam width, wavelength, and Kerr coefficient of the nonlinear material [1]. The limit of $d \to \infty$ corresponds to the well-known Zakharov system, which is a fundamental model in plasma physics (for Langmuir waves) and other fields [36]. The PhC structure is represented by the periodic transverse potential, $V(x) = V_0 \sin^2 x$ ($x$ is normalized so as to make the period equal to $\pi$). Stationary solutions with propagation constant $\mu$ are sought as $\Psi(x,z) = \exp(-i\mu z)\phi(x)$, which gives rise to the stationary version of Eqs. (1) and (2):

$$\mu\phi = -\frac{1}{2}\phi_{xx} + V_0 \sin^2(x)\phi + n\phi, \tag{3}$$

$$n - d\frac{\partial^2 n}{\partial x^2} = |\phi|^2. \tag{4}$$

If the nonlinearity is omitted, Eq. (3) decouples from $n(x)$ and becomes a linear equation, which supports Bloch-wave solutions, $\phi(x) = f(x)\exp(ikx)$, where $k$ is the quasi–wave number and $f(x)$ is a periodic function with period $\pi$. As an example, we take $V_0 = 4$ and display the corresponding dispersion relation, including the lowest three bands, in Fig. 1. From this diagram, it is seen that finite band gaps are introduced by the periodic potential; in particular, the first finite band gap covers a broad interval, $1.305 < \mu < 3.19$.

The nonlinearity may give rise to $x$ periodic modes [37] or localized GSs [38], with $\mu$ falling into the band gaps. Starting with the GS solution in the middle of the gap, we have found different families of bright solitons numerically by using the standard relaxation technique with boundary conditions $\phi(\pm\infty) = 0$. In Fig. 2, we demonstrate generic examples of the GS modes found in the first finite band gap. Local (with $d = 0$) and nonlocal (for $d = 40$) on-site-centered GSs are shown near the bottom of the gap in Figs. 2(a) and 2(d), in the middle of the gap in Figs. 2(b) and 2(e), and close to the top edge in Figs. 2(c) and 2(f), with propagation constants $\mu = 1.31$, $\mu = 2.5$, and $\mu = 3.1$, respectively. The simplest higher order GS solutions of the nonlocal model (off-site-centered solitons) are presented in Figs. 2(g)–2(i). The two distinct types of the solitons, on

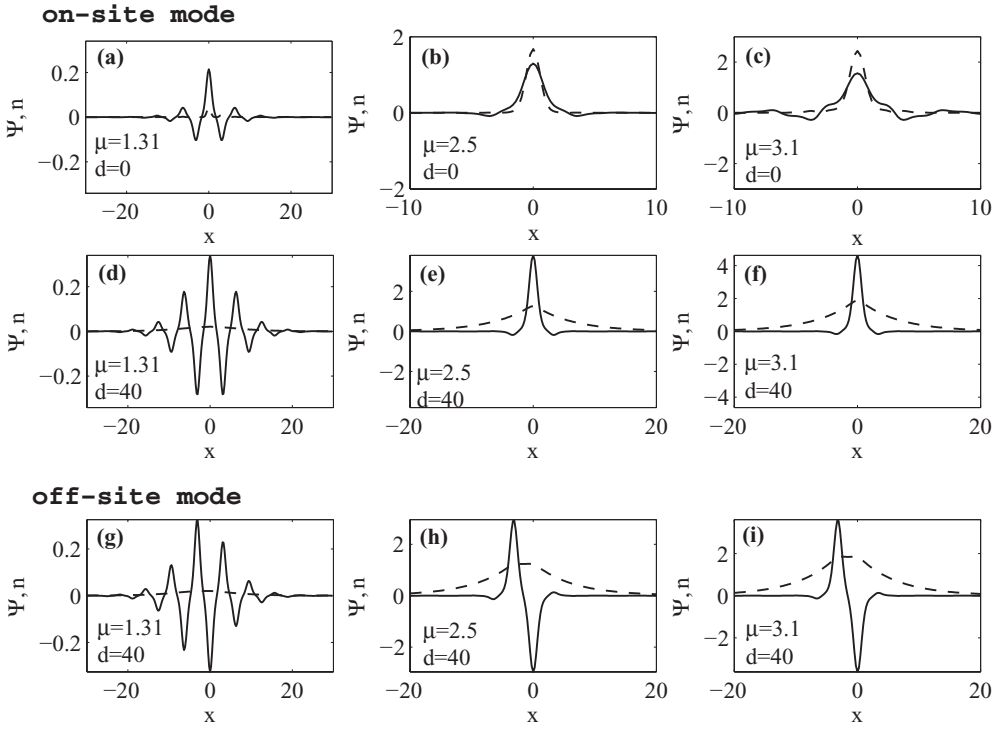


FIG. 2. Typical examples of GS modes in the first finite band gap: (a)–(c) on-site solutions in the local model ($d = 0$), (b)–(f) on-site solutions for $d = 40$, and (h) and (i) off-site solution for $d = 40$. Solid lines show the field profiles, while the corresponding profiles of the RI perturbation, $n(x)$, are plotted by dashed lines.

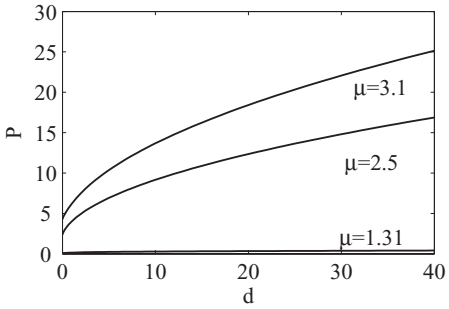


FIG. 3. Total power of on-site GSs vs the nonlocality parameter, $d$, for three distinct values of the propagation constant taken, respectively, near the bottom edge of the first finite band gap's edge ($\mu = 1.31$), in the middle of the gap ($\mu = 2.5$), and approaching the top band edge ($\mu = 3.1$).

site and off site, are defined by the position of their centers with respect to the underlying periodic potential [17,39].

Similar to solitons in nonlocal media with the self-focusing nonlinearity [24,35], the amplitudes of the GSs in the present model increase at a higher degree of the nonlocality, $d$. As a result, the related total power, $\mathbf{P} \equiv \int_{-\infty}^{\infty} |\Psi(x)|^2 dx$, is a growing function of $d$, as shown in Fig. 3. In comparison to the local nonlinear medium, with $d = 0$ [see Figs. 2(a)–2(c)], the width of the RI perturbation, $w_n$, becomes broader with the increase of $d$, for the focusing [24,35] and defocusing signs of nonlinearity alike, due to the diffusion type of the nonlocal response. Relations between $w_n$ and $d$ are shown in the first column of Fig. 4. In contrast to the solitons in self-focusing nonlocal media [17,18], the beam width of the GSs in the present case, $w_b$, *decreases* with the increase of $d$, as shown in the second column of Fig. 4. At very large values of $d$, the beam width in the GS approaches a constant value.

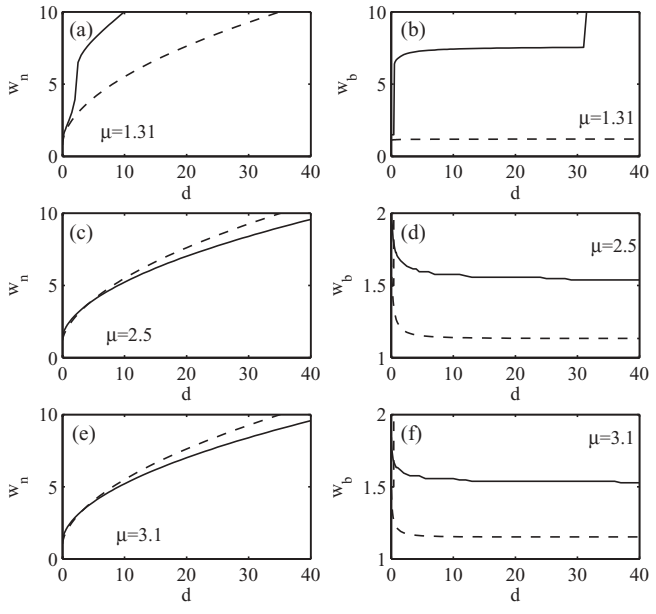


FIG. 4. Left column [(a), (c), and (e)]: the width of the RI profile, $w_n$, in GSs, versus nonlocality parameter $d$. Right column [(b), (d), and (f)]: the width of the field component of the GS, $w_b$, vs $d$. Numerical and variational results are shown by solid and dashed lines, respectively. The value of the propagation constant is fixed in each panel as indicated.

## III. VARIATIONAL APPROXIMATION

It is well known that undulating tails in the shape of GSs, induced by the underlying periodic potential, make the Gaussian ansatz inappropriate as an approximation for GSs, especially close to band-gap edges [33]. However, Fig. 2 demonstrates that the nonlocal nonlinearity makes GSs in the present model more localized, suggesting that they apply to the VA. The Lagrangian density for Eq. (1) is

$$L = \frac{i}{2}(\phi_z^*\phi - \phi_z\phi^*) + k|\phi|^2 + \frac{1}{2}(\phi_x)^2 + V_0\sin^2(x)|\phi|^2 + n|\phi|^2 - \frac{d}{2}(n_x)^2 - \frac{n^2}{2}. \quad (5)$$

Following this argument, we adopt the Gaussian ansatz for field $\phi$ and RI perturbation $n$,

$$\phi(x,z) = A(z)\exp\left[-\frac{x^2}{2w_b^2(z)} + ib(z)x^2\right], \qquad n(x,z) = C(z)\exp\left[-\frac{x^2}{2w_n^2(z)}\right], \quad (6)$$

with $A(z)$, $b(z)$, and $w_b(z)$ standing for the amplitude, chirp, and width of the field component of the GS, whereas $C(z)$ and $w_n(z)$ are the amplitude and width of its RI counterpart. By substituting the ansatz into Lagrangian density (5) and performing the standard calculations [40], we arrive at VA-generated relations between the parameters,

$$\frac{1}{2w_b^2} = \frac{(3d + 2w_n^2)^2}{8w_n^4(2w_n^2 - d)^2} + \frac{\mathbf{P}(3d + 2w_n^2)}{2w_n(d + 2w_n^2)^3} - \frac{2w_n(3d + 2w_n^2)}{(d + 2w_n^2)^2} - (\mu + V_0), \quad (7)$$

$$w_b^2 = \frac{2w_n^2(2w_n^2 - d)}{3d + 2w_n^2}. \quad (8)$$

Using Eqs. (7) and (8), in Fig. 5 we draw the surface plot for the width of the RI profile, $w_n$, as a function of total power $\mathbf{P}$ and nonlocality parameter $d$, at a fixed value of $\mu$, and compare it to the numerical results. As expected, the VA produces good results for the GSs taken in the middle of the band gap, for instance, at $\mu = 2.5$.

In addition, by using the power and propagation constant found numerically in Sec. II, we show in Fig. 4 that both numerical and variation solutions represent the same trend for the widths of both components of the GSs. In particular, for $\mu = 2.5$ and $\mu = 3.1$, as shown in Figs. 4(c)–4(f), $w_n$ increases as the square root of the nonlocality strength, $d$, in agreement with Ref. [32]. In contrast, $w_b$ drops to a finite value as $d$ increases. However, for $\mu = 1.31$, which is very close to the edge of the first finite band gap, the trend is completely different. This difference is explained by the known fact that GSs with the propagation constant taken very close to edges of band gaps are similar to the linear Bloch waves in the linear lattice, as seen in Fig. 2(d). When the amplitude of the

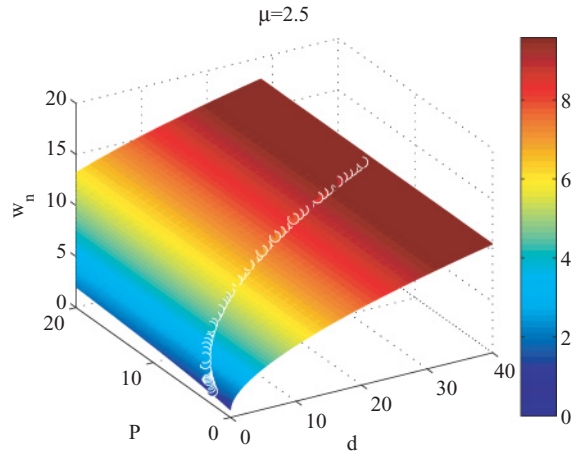


FIG. 5. (Color online) The surface plot for the width of the RI component of the GS, $w_n$, at $\mu = 2.5$, as predicted by variational Eqs. (7) and (8). The chain of dots represents full numerical solutions.

respective undulating tails in the GS shape is comparable to its main peak, the Gaussian ansatz definitely fails. Nevertheless, close to the top edge of the first finite band gap (for instance, at $\mu = 3.1$), the ansatz still works well because the major peak in the GS profile remains much higher than the undulating tails in the entire nonlocality regime. Thus, the applicability condition for the Gaussian-based VA in the system with the self-defocusing nonlocal nonlinearity is clear: It is usable as long as the GS propagation constant is not taken too close to the bottom edge of the first finite band gap.

In the extremely nonlocal regime, the field component in the GSs is much narrower than the RI profile. In this case, the RI profile may be approximated as $n(x) \approx R(x) \equiv e^{-|x|/\sqrt{d}}/(2\sqrt{d})$, where $R(x)$ is the RI response function. The corresponding width of the RI profile is $w_n \approx 2\sqrt{d}\ln 2$. Then, using the quasilinear limit similar to that developed in Ref. [32], one can predict the threshold power necessary for the formation of the GS,

$$\mathbf{P}_{\rm thr} = 2(\mu - \mu_0)\sqrt{d}, \tag{9}$$

where $\mu_0$ is the propagation constant at the edge of the first finite band gap. The comparison to the numerical results in this extremely nonlocal regime is shown in Fig. 6.

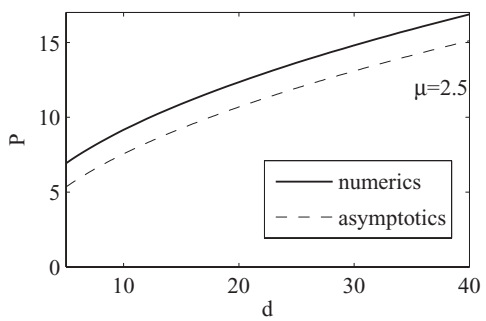


FIG. 6. Threshold power necessary for the formation of the GSs vs the nonlocality parameter, $d$. The solid and dashed lines depict, respectively, the numerical results and asymptotic approximation (9).

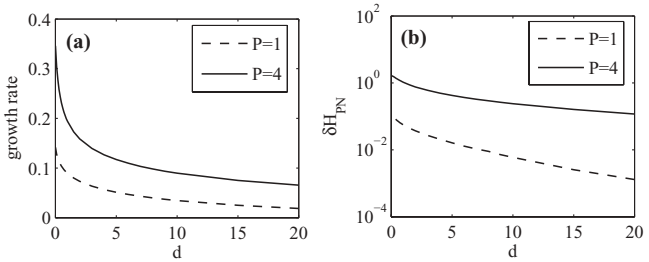


FIG. 7. (a) Instability growth rate and (b) PN energy barrier vs the nonlocality strength, $d$, for different values of the total power, $\mathbf{P}$.

## IV. STABILITY AND MOBILITY OF THE GAP SOLITONS

Having constructed the family of the GSs, we analyze their stability in the usual way, considering perturbed GSs as

$$u = u_0(x)e^{ibz} + \epsilon[p(x)e^{i\delta z} + q(x)e^{-i\delta^* z}]e^{ibz}, \tag{10}$$

$$n = n_0 + \Delta n, \tag{11}$$

where $\epsilon \ll 1$ is the perturbation amplitude, $u_0(x)$ is the unperturbed solution, and $\mathrm{Im}\{\delta\}$ is the growth rate of the perturbations. Although the strengthening nonlocality makes the GS shape sharper and more strongly localized, we have found, somewhat counterintuitively, that the on-site GS family is still stable while its off-site counterpart is not (cf. [13]). Figure 7(a) demonstrates that the nonlocality significantly reduces the growth rate of the unstable perturbation mode for off-site solitons, as in the case of the self-focusing nonlinearity [18]. Due to its diffusion character, the nonlocality smoothes down the undulating tails in the RI profile, $n(x)$. It is this smoothness that stabilizes GSs for either sign of the nonlinearity. Therefore, as the strength of the nonlocality increases, the GS solutions become more stable through the broadening of the effective potential.

The mobility of the GSs in the present model was studied by calculating the respective Peierls-Nabarro (PN) potential barrier, which is defined as the height of an effective periodic potential generated by the underlying lattice. The potential barrier determines the minimum energy needed to move the center of mass of a localized wave packet by one lattice site [41]. As usual, we can calculate the PN barrier as the difference of values of the model's Hamiltonian ($H$) between on-site and off-site modes [17], that is,

$$\delta H = H_{\rm even} - H_{\rm odd}, \tag{12}$$

$$H \equiv \int_{-\infty}^{\infty}\left(-\frac{1}{2}\left|\frac{\partial u}{\partial x}\right|^2 - \frac{1}{2}|u|^2 n - V_x|u|^2\right)dx. \tag{13}$$

As seen in Fig. 7(b), in the first finite band gap the PN barrier is reduced in comparison to the case of the local nonlinearity, $d = 0$, which is a natural manifestation of the nonlocality.

## V. CONCLUSION

We have reported the analysis of the existence, stability, and mobility of one-dimensional GSs in the periodic potential structure combined with the self-defocusing nonlocal nonlinearity. We have found that the GSs become more tightly localized in space, with a higher formation-power

threshold. The results have been obtained in numerical form and reproduced, with a reasonable accuracy, by the VA. Using the linear-stability analysis and calculating the PN potential barrier, we have demonstrated that the GSs become not only more stable but also more mobile with the increase of the nonlocality. The comparison with the limit of the extreme nonlocality was reported too. Taking into regard the possibilities offered by the currently available technology for fabricating nonlocal nonlinear media with controllable properties, such as photorefractive crystals, nematic liquid crystals, and thermo-optical materials, the results reported in this work may suggest new possibilities for the design of soliton-based photonic devices. For instance, photorefractive materials like SBN or $LiNbO_3$ [42] or liquid-filled photonic crystal fibers [43] may serve as experimental platforms to realize our proposed configuration with a self-defocusing nonlinearity and periodic index modulations. It may also be interesting to extend the model and the analysis of GSs in it (including vortex solitons) to two-dimensional geometry.

## ACKNOWLEDGMENTS

This work is partly supported by the National Science Council of Taiwan with contrasts NSC 95-2112-M-007-058-MY3, NSC 95-2120-M-001-006, and NSC 98-2112-M-007-012.

[1] Y. S. Kivshar and G. P. Agrawal, *Optical Solitons: From Fibers to Photonic Crystals* (Academic, San Diego, CA, 2003), and references therein.
[2] A. D. Boardman and A. P. Sukhorukov, eds., *Soliton-Driven Photonics*, NATO Science series, II Mathematics, Physics and Chemistry, Vol. 33 (Kluwer Academic Publishers, Dordrecht, the Netherlands, 2001).
[3] J. D. Joannopoulos, R. D. Meade, and J. N. Winn, *Photonic Crystals: Molding the Flow of Light* (Princeton University Press, Princeton, NJ, 1995).
[4] C. M. de Sterke and J. E. Sipe, in *Progress in Optics*, edited by E. Wolf (North-Holland, Amsterdam, 1994), Vol. 33, p. 203.
[5] S. F. Mingaleev and Y. S. Kivshar, Phys. Rev. Lett. **86**, 5474 (2001).
[6] R. Slusher and B. Eggleton, eds., *Nonlinear Photonic Crystals* (Springer-Verlag, Berlin, 2003).
[7] E. A. Ostrovskaya and Y. S. Kivshar, Phys. Rev. Lett. **90**, 160407 (2003).
[8] B. J. Eggleton, R. E. Slusher, C. M. de Sterke, P. A. Krug, and J. E. Sipe, Phys. Rev. Lett. **76**, 1627 (1996).
[9] N. K. Efremidis, S. Sears, D. N. Christodoulides, J. W. Fleischer, and M. Segev, Phys. Rev. E **66**, 046602 (2002).
[10] M. Peccianti, K. A. Brzdkiewicz, and G. Assanto, Opt. Lett. **27**, 1460 (2002).
[11] V. A. Brazhnyi and V. V. Konotop, Mod. Phys. Lett. B **18**, 627 (2004).
[12] B. Eiermann, T. Anker, M. Albiez, M. Taglieber, P. Treutlein, K.-P. Marzlin, and M. K. Oberthaler, Phys. Rev. Lett. **92**, 230401 (2004).
[13] D. E. Pelinovsky, A. A. Sukhorukov, and Y. S. Kivshar, Phys. Rev. E **70**, 036618 (2004).
[14] H. Sakaguchi and B. A. Malomed, J. Phys. B **37**, 1443 (2004); **37**, 2225 (2004).
[15] D. N. Christodoulides, F. Lederer, and Y. Silberberg, Nature (London) **424**, 817 (2003).
[16] Y. V. Kartashov, V. A. Vysloukh, and L. Torner, Phys. Rev. Lett. **93**, 153903 (2004).
[17] Z. Xu, Y. V. Kartashov, and L. Torner, Phys. Rev. Lett. **95**, 113901 (2005).
[18] Y. Y. Lin, I.-H. Chen, and R.-K. Lee, J. Opt. A: Pure Appl. Opt. **10**, 044017 (2008).
[19] W. Królikowski and O. Bang, Phys. Rev. E **63**, 016610 (2000).
[20] G. C. Duree, J. L. Shultz, G. J. Salamo, M. Segev, A. Yariv, B. Crosignani, P. DiPorto, E. J. Sharp, and R. R. Neurgaonkar, Phys. Rev. Lett. **71**, 533 (1993).
[21] C. Conti, M. Peccianti, and G. Assanto, Phys. Rev. Lett. **91**, 073901 (2003).
[22] C. Rotschild, O. Cohen, O. Manela, M. Segev, and T. Carmon, Phys. Rev. Lett. **95**, 213904 (2005).
[23] N. K. Efremidis, Phys. Rev. A **77**, 063824 (2008).
[24] W. Królikowski, O. Bang, N. I. Nikolov, D. Neshev, J. Wyller, J. J. Rasmussen, and D. Edmundson, J. Opt. B: Quant. Semiclass. Opt. **6**, S288 (2004).
[25] S. Lopez-Aguayo, A. S. Desyatnikov, and Y. S. Kivshar, Opt. Express **14**, 7903 (2006).
[26] Y. Y. Lin, R.-K. Lee, and Y. S. Kivshar, J. Opt. Soc. Am. **25**, 576 (2008).
[27] O. Bang, W. Królikowski, J. Wyller, and J. J. Rasmussen, Phys. Rev. E **66**, 046619 (2002).
[28] M. Peccianti, K. A. Brzdkiewicz, and G. Assanto, Opt. Lett. **27**, 1460 (2002).
[29] Z. Xu, Y. V. Kartashov, and L. Torner, Opt. Lett. **30**, 3171 (2005).
[30] Y. Y. Lin, R.-K. Lee, and B. A. Malomed, Phys. Rev. A **80**, 013838 (2009).
[31] Y. Y. Lin and R.-K. Lee, Opt. Express **15**, 8781 (2007).
[32] A. W. Snyder and D. J. Mitchell, Science **276**, 1538 (1997).
[33] A. Gubeskys, B. A. Malomed, and I. M. Merhasin, Stud. Appl. Math. **115**, 255 (2005).
[34] S. Adhikari and B. A. Malomed, Europhys. Lett. **79**, 50003 (2007).
[35] W. Królikowski, O. Bang, J. J. Rasmussen, and J. Wyller, Phys. Rev. E **64**, 016612 (2001).
[36] V. E. Zakharov, Z. Eksp. Teor. Fiz. **62**, 1745 (1972) [Sov. Phys. JETP **35**, 908 (1972)]; E. I. Shulman, Dokl. Akad. Nauk SSSR **259**, 578 (1981); L. Stenflo, Phys. Scr. **33**, 156 (1986).
[37] Y. Y. Lin, R.-K. Lee, Y.-M. Kao, and T.-F. Jiang, Phys. Rev. A **78**, 023629 (2008).
[38] Y. Zhang and B. Wu, Phys. Rev. Lett. **102**, 093905 (2009).
[39] B. J. Dabrowska, E. A. Ostrovskaya, and Y. S. Kivshar, J. Opt. B: Quantum Semiclass. Opt. **6**, 423 (2004).
[40] B. A. Malomed, in *Progress in Optics*, edited by E. Wolf (North-Holland, Amsterdam, 2002), Vol. 43, p. 71.
[41] Y. S. Kivshar and D. K. Campbell, Phys. Rev. E **48**, 3077 (1993).
[42] N. Zhu, R. Guo, S. Liu, Z. Liu, and T. Song, J. Opt. A: Pure Appl. Opt. **8**, 149 (2006).
[43] C. R. Rosberg, F. H. Bennet, D. N. Neshev, P. D. Rasmussen, O. Bang, W. Krolikowski, A. Bjarklev, and Y. S. Kivshar, Opt. Express **15**, 12145 (2007).